International Journal of Modern Research in Engineering and Technology (IJMRET)
www.ijmret.org Volume 5 Issue 2 ǁ March 2020.

Comparison of Pressure Results between Wind Tunnel and CFD Simulation for University Baghdad Tower Building

Karrar Waleed Saeed* Shaymaa Abdul Muttaleb** Jassim Muhsin***

Mustansiriyah University, College of Engineering ,Civil Department

Baghdad – Iraq

Abstract: *High-rise buildings located in the high velocity wind regions are highly vulnerable to large pressures. Pressure on high-rise building is studied in this current paper. CFD model was completed in (3D) ANSYS (Fluid Fluent). Using finite volume method to predict the wind pressures on high-rise building using specified boundary conditions. RNG k-ε turbulence model was used in the software to consider the wind turbulence. Present numerical approach was proved by comparison the pressure results for different wind speed and wind angle with experimental wind tunnel tests. This valid CFD model was applied in the simulation of the wind analysis for University Baghdad tower, which is located in Baghdad City, Iraq. It is concluded that wind pressure results for wind tunnel test have a very good agreement with the wind pressure results of CFD for different velocity and wind angle. Numerical analysis can be used instead of examining the costly wind tunnel.*

Keywords: *high-rise buildings, finite volume method, computational fluid dynamic (CFD), RNG κ-ε turbulence model, wind pressure on building, wind tunnel test.*

I. Introduction

From the early times of civilization, buildings as well as tall towers smitten the humankind, the structure for such constructions were used to protect and then for ecclesiastical uses. The rapid elevation in the growth regarding modern constructions of tall buildings that started in the 1880s, was mainly for residential as well as for commercial uses. High-rise commercial buildings have been majorly considered as response to demands through businesses for being close with each other, along city centers, as achievable, thus providing extreme pressure on existing land spaces. Furthermore, due to the fact that they are forming unique landmarks, the tall commercial buildings have been often created in the city center in the sort of standing symbols with regard to the corporate organizations [5]. Certain improvements in novel techniques of construction in twentieth century established structures which are considered to be fairly lightweight, low damping, as well as flexible, that might be exposing the structures to the impact of wind actions. Wind engineering can be considered as a field with the goal of majorly creating tools for better understanding regarding the fluid's action on structures with the origins, which might be marking out to 1960s. Improving the understanding with regard to this presented work encouraged the structural engineers for designing as well as ensuring the structure's performance with is the subject to wind's action to be in proper limits throughout the structure's lifetime in the structural safety as well as the serviceability criteria[6]. There have been many approaches to analyze tall buildings with regard to the wind load after utilizing building codes, wind tunnel or numerical analysis using the software. [3]Examined the impact of wind flow around 3D buildings with CFD. Steady Navier-Stokes equation was solved with k-ε turbulence model in the simulation. Power-law velocity profile has been utilized to describe the incident wind. There are four flows were specified in this work and simulation results have been put to comparison with full-scale wind tunnel data. Based on such comparison, it has been specified that there has been accordance with regard to outputs, which are confirming the wind flow's validation via CFD. [7]Suggested wind pressure on the flat roof regarding high-rise building. Reynolds average Navier stoke equation with standard k-ε turbulence model was utilized in the modeling. The wind blowing has been suggested to be in oblique and normal directions. The estimation regarding wind pressure for three distinctive distance from roof edges to first grid line's center. The results specified that the roof surface might be classified in to two subregions based on computed pressure. Furthermore, it has been indicated that oblique direction that is related to the wind blowing affected more than normal direction in the pressure calculations. [8]Investigated the modeling regarding the wind load on the tall buildings with the use of CFD. Turbulence has been provided at inlet via simulation with the use of LES with RNG-based sub grid-scale viscosity model. The dimensions of the model were (76.2x76.2x635 mm) and the computational domain dimensions were (32.5D x 15D x 3H). When compared those obtained from wind tunnel tests with CFD wind force and the moment spectra showed that an agreement between the CFD and physical simulations, and accomplished that CFD wind tests on tall buildings were a possible stand by to the conventional tests in wind tunnels. [2]Examined comparison related to the wind load on building used design codes, wind tunnel tests and CFD. Two building models were used in this study. The dimensions of the two building were (25x15x45 m) and (55x45x200 m). After calculated the wind loads on buildings. he concluded that the estimated wind loads on buildings by using CFD is comparable with the results by wind tunnel test and those by building design codes are more conservative than the CFD and wind tunnel test. [9]Provided major theoretical background with regard to utilizing CFD for the wind boundary layer simulations as well as suitable approaches specified to generate domains and meshes for the models of CFD. In addition, it showed many empirical approaches which could be utilized as boundary conditions with the lack of data that has high accuracy for simulation. CFD simulation results of pressure distribution (112m) high-rise building has been put to comparison with wind tunnel tests results and indicated the performance regarding such experimental approaches have been acceptable.[4] Examined the analysis regarding high-rise buildings, which has been determined for various models of turbulent with the use of CFD and put to comparison with experimental results acquired from Tokyo Polytechnic University. A 2-D rectangular building model, which has the dimensions (0.1mx0.2m) in the plan, were specified for numerical simulations. The direction of wind has been specified in various angles with building walls as 0^o, 45^o& 90^o. The wind pressure coefficients acquired from such analysis with the use of different turbulent models have been put to comparison with wind pressure coefficients acquired from wind tunnel experiments. They have indicated that the ST k-ω turbulence model as well as the realizable k-ε turbulence model have been more efficient from the acquired results, and could examined wind forces on high raised rectangular buildings with the use of CFD simulations for various angles in the SST k-ω turbulence model as well as the realizable k-ε turbulence model. [10] studied a wind pressure on (406m) tall slender structure with circular cross-section by using CFD, which was complimented with experimental data obtained via wind tunnel testing. They were used RANS turbulence models to obtain the pressure distribution and flow behaviour of the structure. The comparison between the all methods by using pressure coefficient Cp. They were shown that RANS turbulence models were adequate to predict wind induced loads for buildings and the pressure variations on the windward, leeward and crosswind faces indicated an agreement with experimental data. The results were shown that the CFD simulations provide a reasonable estimate with less computational cost when compared with wind tunnel experimentation, and Overall k-ω provided good estimates compared with experimental data where in most cases the difference between both were less than 10% and at maximum cases (leeward face) less than 30%.

The Governing Equations of Fluid

The governing equations in fluid dynamics can be applied to wind flow. Liquid or wind flows in CFD codes are governed by partial differential equations, which are based on the conservation laws for mass, energy and momentum. The following expressions are applied for three dimensional, steady and incompressible flows with constant viscosity.

$\frac{\partial\rho}{\partial t}+\left[\frac{\partial(\rho u)}{\partial x}+\frac{\partial(\rho v)}{\partial y}+\frac{\partial(\rho w)}{\partial z}\right]=0$ Continuity equation (1)

$\rho\frac{Du}{Dt}=-\frac{\partial\rho}{\partial x}+\frac{\partial\tau_{xx}}{\partial x}+\frac{\partial\tau_{yx}}{\partial y}+\frac{\partial\tau_{zx}}{\partial z}+\rho f_x$ Momentum equation (2-x)

$\rho\frac{Dv}{Dt}=-\frac{\partial\rho}{\partial y}+\frac{\partial\tau_{yy}}{\partial y}+\frac{\partial\tau_{yx}}{\partial x}+\frac{\partial\tau_{zy}}{\partial z}+\rho f_y$ Momentum equation (2-y)

$\rho\frac{Dw}{Dt}=-\frac{\partial\rho}{\partial z}+\frac{\partial\tau_{zz}}{\partial z}+\frac{\partial\tau_{yz}}{\partial y}+\frac{\partial\tau_{zx}}{\partial x}+\rho f_z$ Momentum equation (2-z)

$$\tau_{xy}=\tau_{yx}=\mu(\frac{\partial v}{\partial x}+\frac{\partial u}{\partial y})$$

$$\tau_{xz}=\tau_{zx}=\mu(\frac{\partial w}{\partial x}+\frac{\partial u}{\partial z})$$

$$\tau_{zy}=\tau_{yz}=\mu(\frac{\partial v}{\partial y}+\frac{\partial w}{\partial y})$$

$$\tau_{xx}=-\frac{2}{3}\mu(\nabla.V)+2\mu\frac{\partial u}{\partial x}$$

$$\tau_{yy}=-\frac{2}{3}\mu(\nabla.V)+2\mu\frac{\partial v}{\partial y}$$

$$\tau_{zz}=-\frac{2}{3}\mu(\nabla.V)+2\mu\frac{\partial w}{\partial z}$$

$$\rho\frac{D}{Dt}\left(e+\frac{V^2}{2}\right)=\rho q+\frac{\partial}{\partial x}\left(k\frac{\partial T}{\partial x}\right)+\frac{\partial}{\partial y}\left(k\frac{\partial T}{\partial y}\right)+\frac{\partial}{\partial z}\left(k\frac{\partial T}{\partial z}\right)-\frac{\partial(up)}{\partial x}$$

$-\frac{\partial(vp)}{\partial y}-\frac{\partial wp}{\partial z}+\frac{\partial(u\tau_{xx})}{\partial x}+\frac{\partial(u\tau_{yx})}{\partial y}+\frac{\partial(u\tau_{zx})}{\partial z}+\frac{\partial(v\tau_{xy})}{\partial x}+\frac{\partial(v\tau_{yy})}{\partial y}+\frac{\partial(v\tau_{zy})}{\partial z}+\frac{\partial(w\tau_{xz})}{\partial x}+\frac{\partial(w\tau_{yz})}{\partial y}+\frac{\partial(w\tau_{zz})}{\partial z}+$
$\rho f.V$ Energy equation (3)

Where; $\boldsymbol{\rho}$ is density of fluid in Kg/m^3, $\boldsymbol{u}$, $\boldsymbol{v}$ and $\boldsymbol{w}$ velocities of fluid in x, y and z directions respectively in m/s, $\boldsymbol{\tau}$ is the shear stress in Pa, $\boldsymbol{t}$ is the time in s, f_x, f_y and f_z are the body forces in N, $\boldsymbol{\mu}$ is the molecular viscosity coefficient in Pa.s, $\boldsymbol{V}$ is velocity vector in m/s, $\boldsymbol{k}$ is the thermal conductivity, $\boldsymbol{e}$ is the internal energy inJ,Tis the temperature in C^o and $\boldsymbol{q}$ is the heat transferred*W/m²·K*.

RNG k- ε Model

Based on a mathematical technique of renormalization group, which is proposed by [11], this model is utilized to renormalize the Navier-Stokes equations and to put the effects of smaller scales of motion into account. In contrast to the standard k-ε turbulence model, the eddy viscosity is determined from a single turbulence length scale.

a) Transport equation for kinetic energy ***k***:

$\rho\frac{\partial k}{\partial t}=\frac{\partial}{\partial x_i}\left[\alpha_k\mu_{eff}\frac{\partial k}{\partial x_i}\right]-P_k+\rho\varepsilon$(4)

b) Transport equation for dissipation rate **ε**:

$$\rho \frac{\partial \varepsilon}{\partial t} = \frac{\partial}{\partial x_i}\left[\alpha_\varepsilon \mu_{eff} \frac{\partial \varepsilon}{\partial x_i}\right] - C_{1\varepsilon}\frac{\varepsilon}{k} P_k + C^*_{2\varepsilon}\frac{\varepsilon}{k}\rho\varepsilon (5)$$

Where,

$$\mu_{eff} = \mu + \mu_t (6)$$

$$\mu_t = \rho C_\mu \frac{k^2}{\varepsilon} (7)$$

Where; $C_\mu = 0.0845, \alpha_k = \alpha_\varepsilon = 1.39, C_{1\varepsilon} = 1.42, C_{2\varepsilon} = 1.68$

The significant difference **(6)** between both Standard and RNG k-ε turbulence models is calculated from the near wall turbulence data as hereunder:

$$C^*_{2\varepsilon} = C_{2\varepsilon} - \frac{C_\mu \rho \eta^3 (1 - \frac{\eta}{\eta_o})}{1 + \beta\eta^3} (8)$$

Where;

$$\eta = \frac{k}{\varepsilon}\sqrt{2 S_{ij} . S_{ij}} (9)$$

$$S_{ij} = \frac{1}{2}\left(\frac{\partial u_i}{\partial x_j} + \frac{\partial u_j}{\partial x_i}\right) (10)$$

$$\eta_o = 4.377$$

$$\beta = Wall\ damping, needs\ to\ be\ applied\ to\ ensure\ the\ viscosity = 0.01.$$

$\boldsymbol{\rho}$ = the density of air, $\boldsymbol{u_i}$, $\boldsymbol{u_j}$ the velocity components, $\boldsymbol{P}$ is the pressure of air in Pa, $\boldsymbol{\mu}$ is the dynamic viscosity, $\boldsymbol{t}$ is the time, $\boldsymbol{i}$, $\boldsymbol{j}$ are 1, 2, 3.

Experimental Work

The building, known as the "Baghdad University tower'', is one of the tallest buildings in the capital, Baghdad University, near the Jadriyah Bridge. Designed by the German (Walter Kropis, 1957) as shown in the (**Plate 1**). Baghdad University Tower consists of 20 floors. The dimensions of the tower are (27.45 x 24.69 x 82.74) meters. The wind tunnel scale was chosen to be 1:140 as that is typical in industry practice to use this factor in studies. In the case of the chosen scale for building, the dimensions became (196 x 176 x 591) mm as seen in (**Figure 1**). The experimental model is manufactured from wood. The wood plate connection seams were filled with wood putty to ensure smooth wind flow over the seams. The model is open from the base for in order to allow the introduction of tubes to measure air pressure measuring tubes. Eighteen pressure ports are made on the each faces of tower model building for measurement of wind pressures as are shown in (**Figure 1**) and the locations of pressure ports on faces of tower model are shown in the **Table** (**1**) and (**2**). The number and location of pressure ports for opposite faces for tower model are same. Wind direction on model as shown in the (**Figure 2**). The laboratory-building tower model that has been used in experimental is shown in (**Plate 2**).

Plate (1) Real University Baghdad Tower.

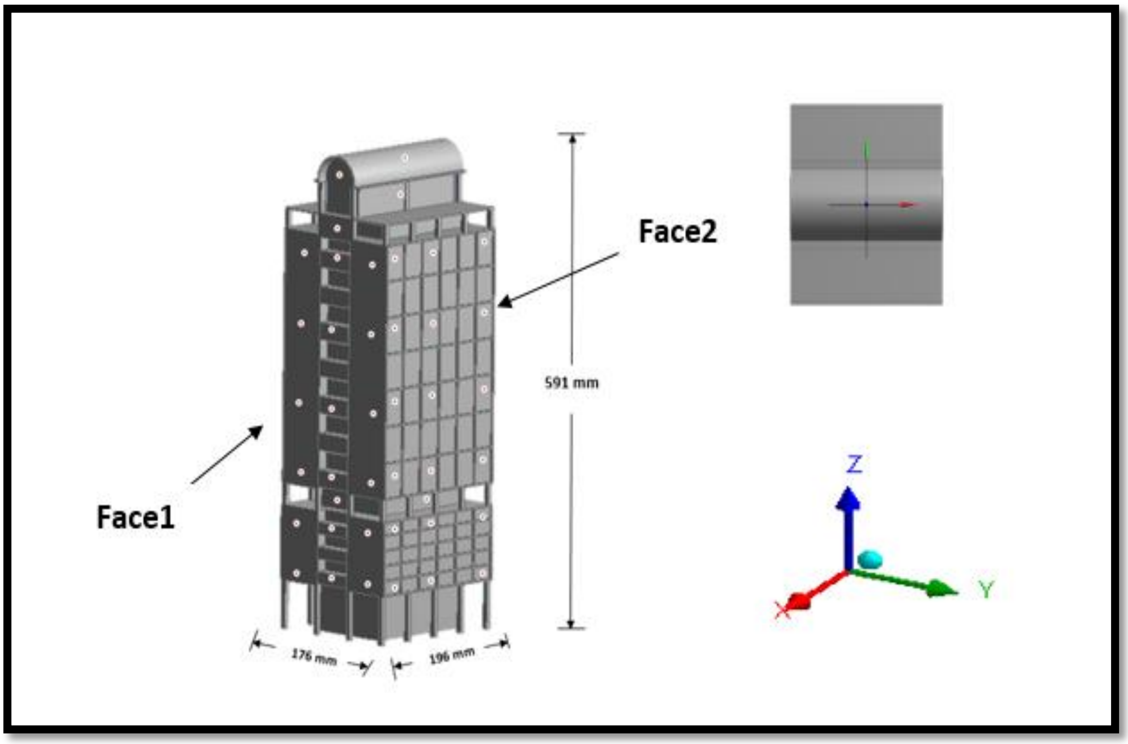

Figure (1) The Dimensions and Pressure Ports of University Baghdad Tower Model.

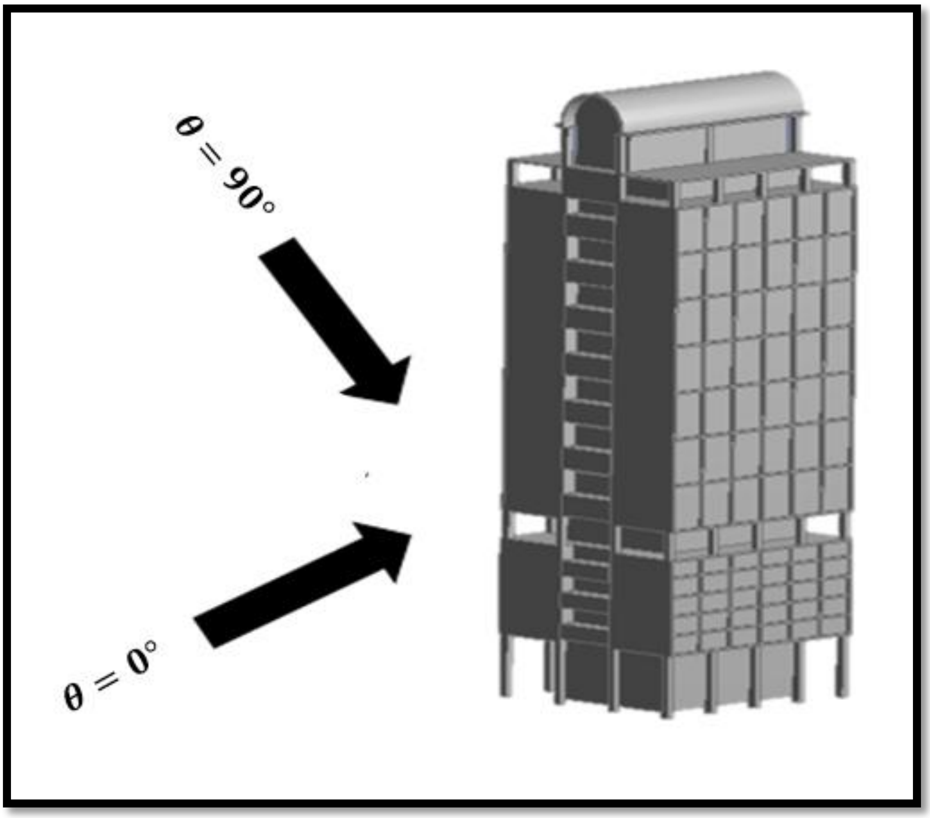

Figure (2) Wind Directions on Model.

Table (1) Pressure Port Numbers and Locations for Face1 of Baghdad University Tower Model.

Point Number	X [mm]	Y [mm]	Z [mm]
1	98	-70	70
2	98	0	70
3	98	70	70
4	98	-70	135
5	98	0	135
6	98	70	135
7	75	0	170
8	98	-70	240
9	98	0	240
10	98	70	240
11	98	-70	375
12	98	0	375
13	98	70	375
14	98	-70	470
15	98	0	470
16	98	70	470
17	98	0	505
18	90	0	570

Table (2) Pressure Port Numbers and Locations for Face2 Baghdad University Tower Model.

Point Number	X [mm]	Y [mm]	Z [mm]
1	-85	88	70
2	-10	88	70
3	85	88	70
4	-85	88	145
5	-10	88	145
6	85	88	145
7	-10	60	170
8	-85	88	250
9	-10	88	250
10	85	88	250
11	-85	88	385
12	-10	88	385
13	85	88	385
14	-85	88	475
15	-10	88	475
16	85	88	475
17	-10	60	505
18	0	35	580

Plate (2) Photographs Showing the Laboratory Horizontal Wind Tunnel University Baghdad Tower Model.

This low speed open circuit wind tunnel has been designed, manufactured and constructed at the Mechanical Engineering Department at Baghdad University - College of Engineering. The work is one of the pioneer projects adapted by the R & D Office at the Iraqi MOHESR. The flow cross-section WxH: 700x700 mm and with length 1500 mm as shown in (**Figure 3**). The wind velocity was varying from 1 to 70 m/s.

The bed and sidewalls of wind tunnel are made from wood. Every model is placed in the wind tunnel at the center of the measurement section. The wind velocity used in the test is 30, 40 and 50 m/s.

Figure (3) Photographs Showing the Laboratory Wind Tunnel.

CFD Simulation Part

The optimum mesh sizes that selected to be adequately modeled the wind flow over building model was having 1 mm for edges and 5 mm for face.Theboundary conditions of the building modelis shown (**Figure 4**) .The unstructured mesh scheme is applied in this paper as shown (**Figure 5**). The number of cells for building model is about $11x10^5$. The number of iteration is 5000.

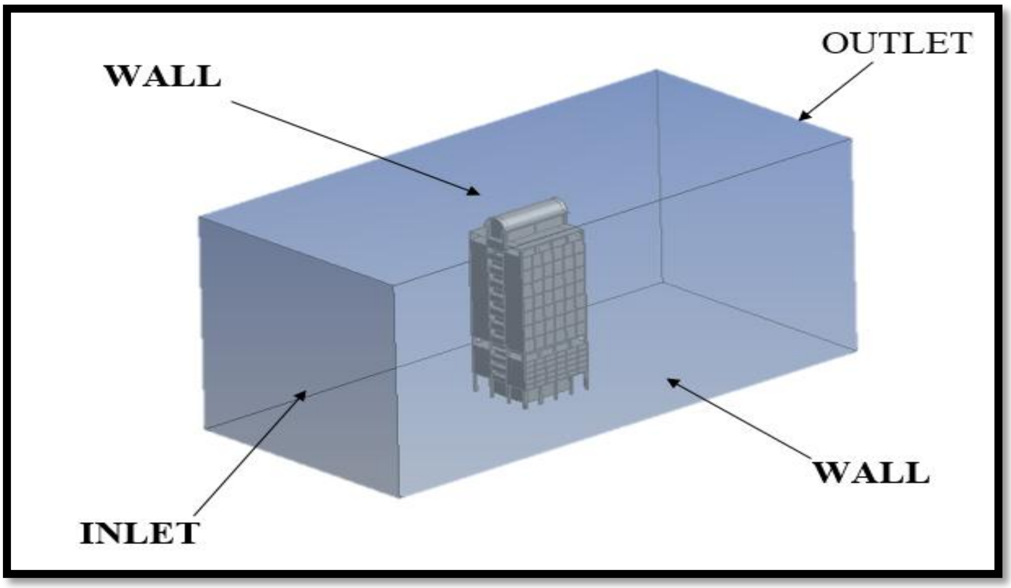

Figure (4) the Boundary Conditions of the Model Study.

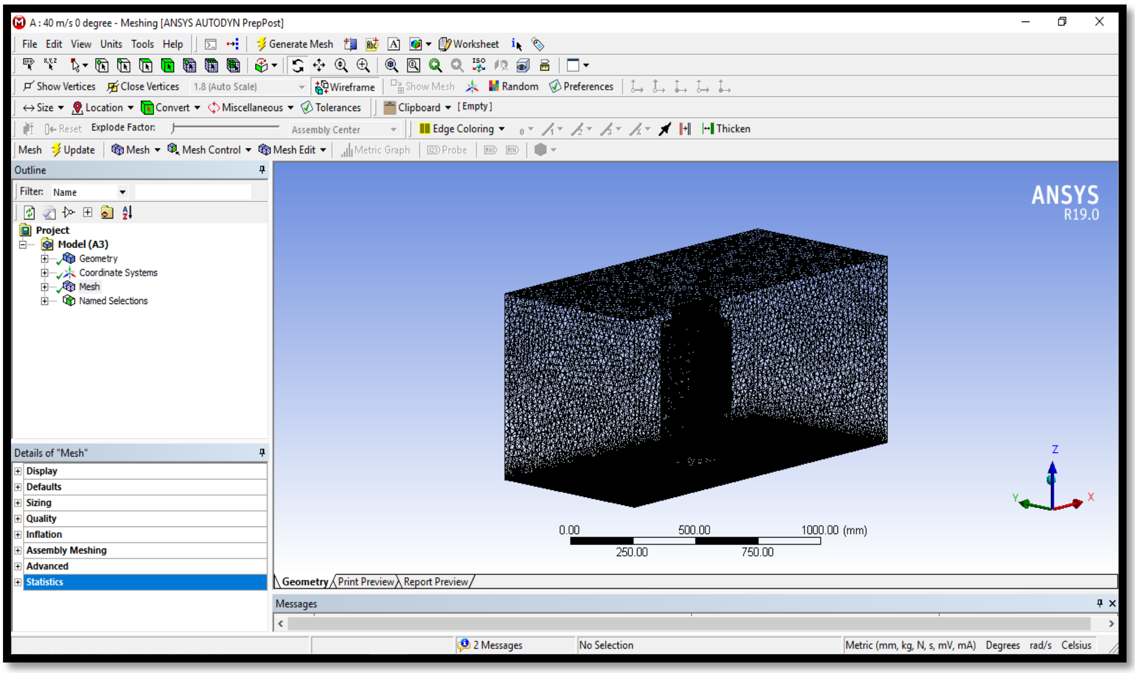

Figure (5) Mesh Generation.

Pressure Results and Discussion for University Baghdad Tower

Figure (6),**(8)** and**(10)** indicated the results of pressure for windward1, while **Figure (7)**, **(9)** and**(11)** shown the results of pressure for leeward1 with angle of wind 0 degree, while **Figure (12)**,**(14)** and**(16)** indicated the results of pressure for windward2, while **Figure (13)**, **(15)** and**(17)** shown the results of pressure for leeward1 with angle of wind 90 degree.All these for different value of wind velocity (30, 40 and 50 m/s).**Figure (18)**shown the pressure contour results for model, while **Figure (19)** shown the velocity streamline for model. Relative errors for the pressure between numerical and experimental results are generally For University Baghdad tower model is 0.18% to 6.17%.It can be seen from figures below of velocity streamline distribution for model that the wind speed on the real side is the same on the hypothetical side and starts to change when exposed to resistance.It can be showed that the wind distribution on the University Baghdad tower model shows a strong change in speed as the shape of the tower increases friction with wind and makes the change in speed so large.

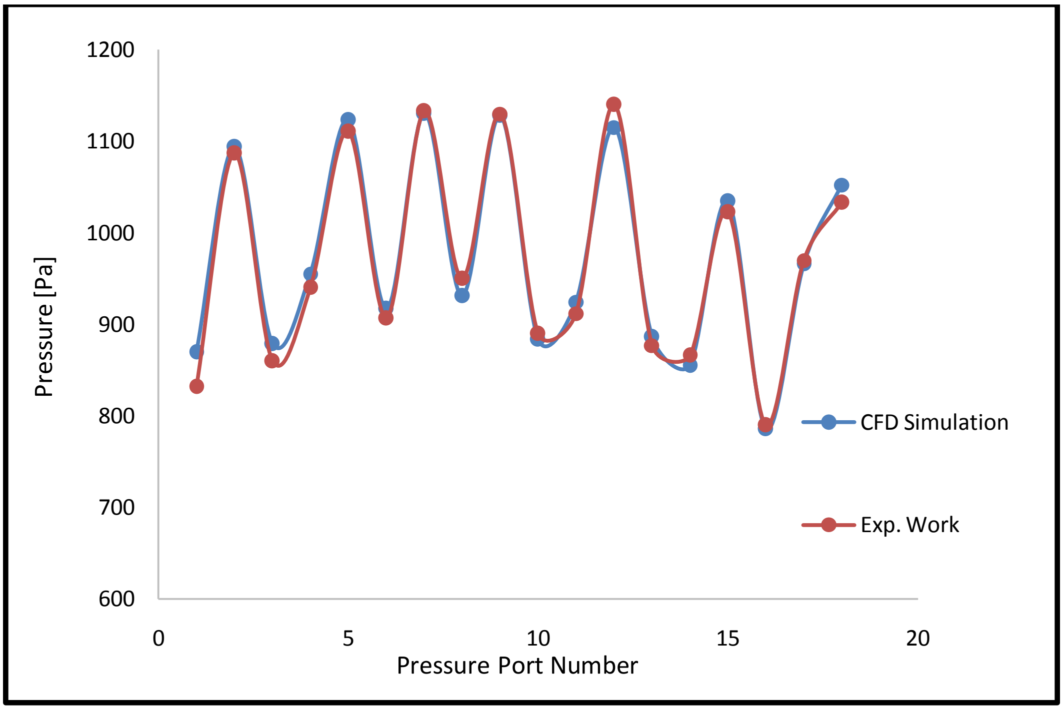

Figure (6) Comparison between Pressures Obtained by Experimental and Numerical Models for Windward1 Model for Wind Velocity 30 m/s with angle of wind 0 degree.

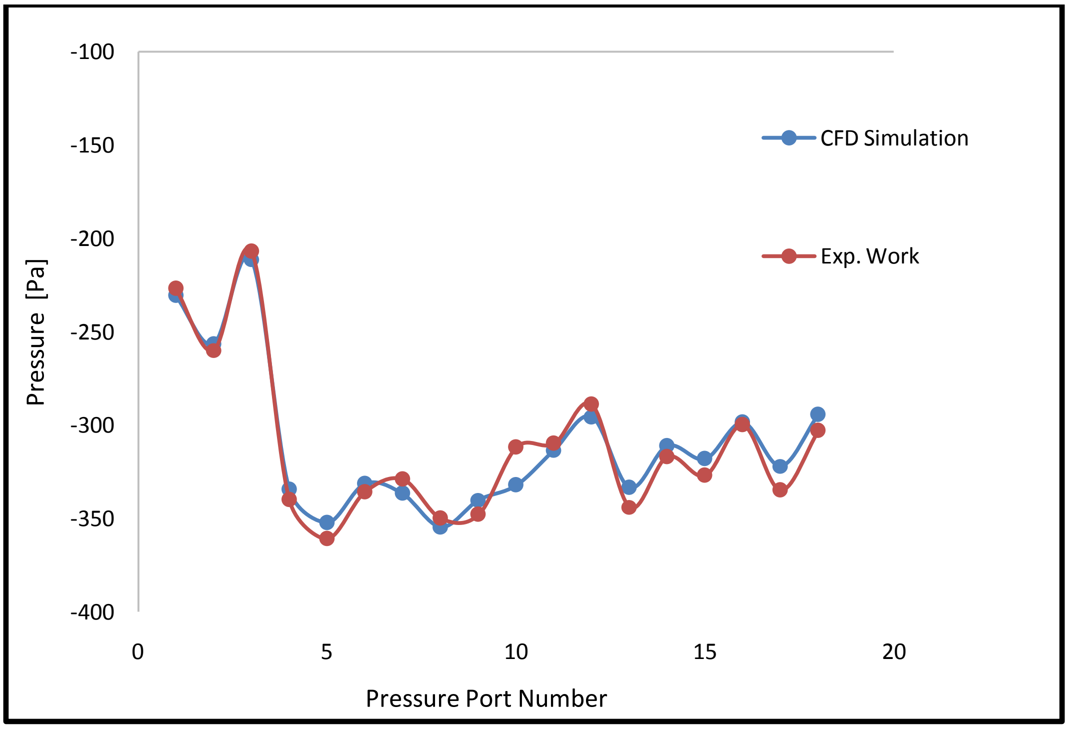

Figure (7) Comparison between Pressures Obtained by Experimental and Numerical Models for Leeward1 Model for Wind Velocity 30 m/s with angle of wind 0 degree.

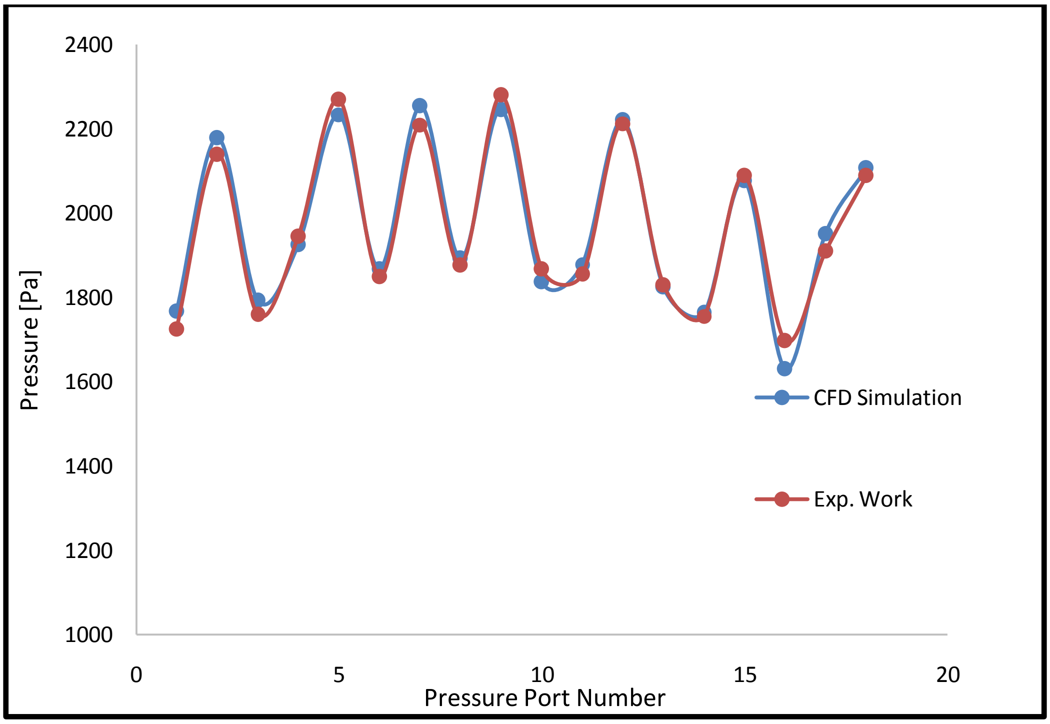

Figure (8) Comparison between Pressures Obtained by Experimental and Numerical Models for Windward1 Model for Wind Velocity 40 m/s with angle of wind 0 degree.

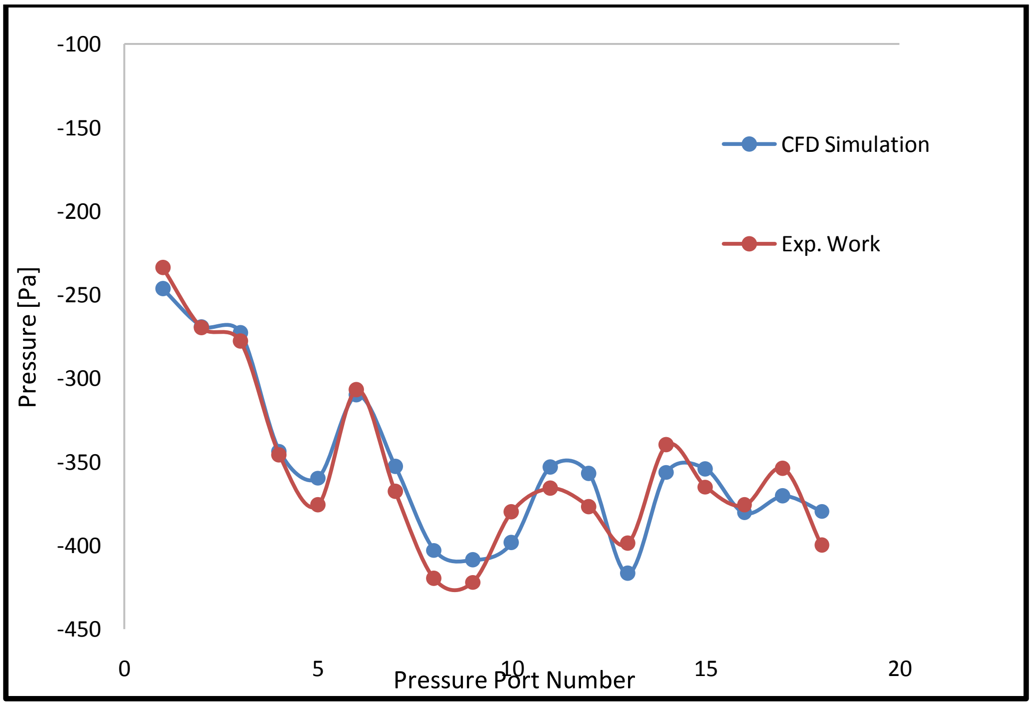

Figure (9) Comparison between Pressures Obtained by Experimental and Numerical Models for Leeward1 Model for Wind Velocity 40 m/s with angle of wind 0 degree.

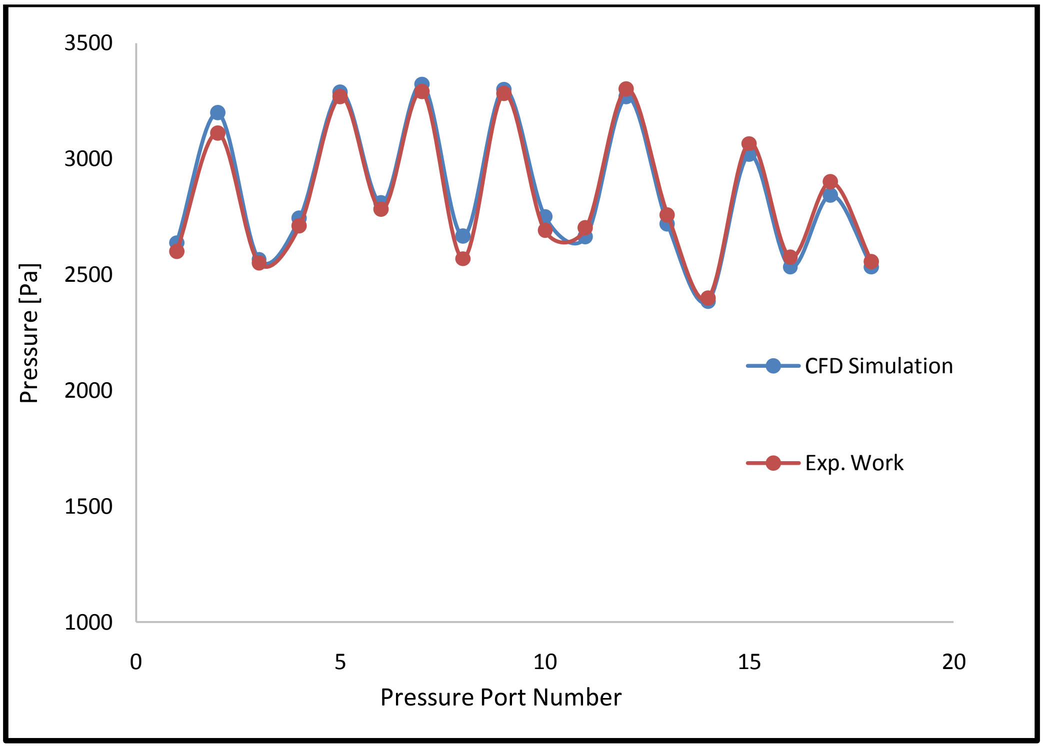

Figure (10) Comparison between Pressures Obtained by Experimental and Numerical Models for Windward1 Model for Wind Velocity 50 m/s with angle of wind 0 degree.

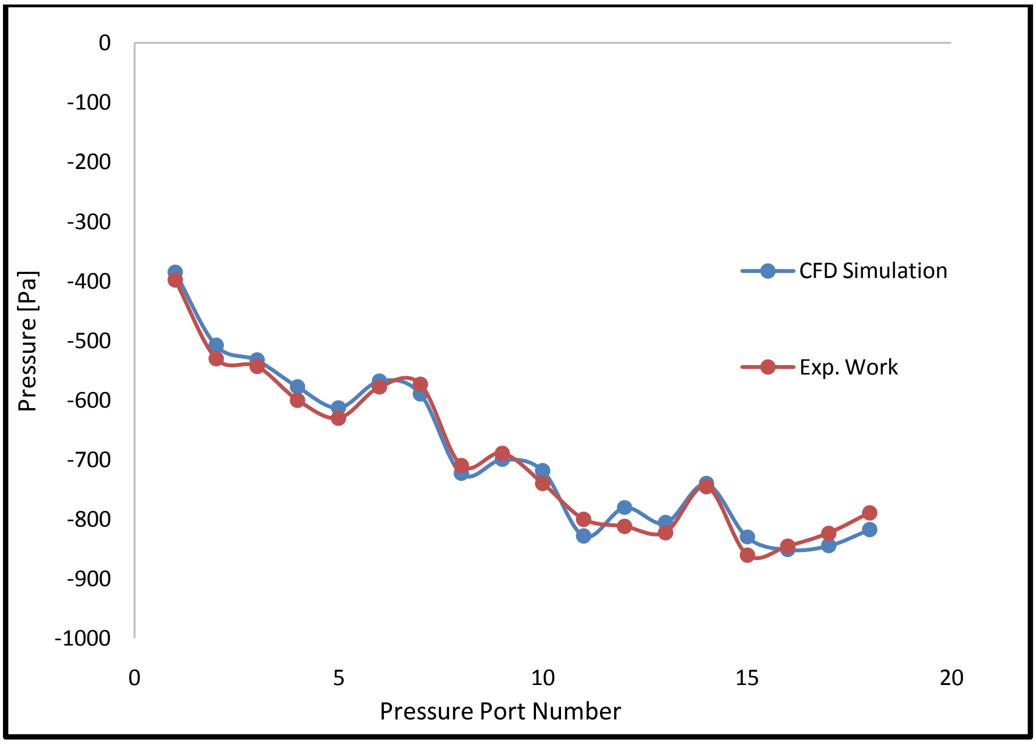

Figure (11) Comparison between Pressures Obtained by Experimental and Numerical Models for Leeward1 Model for Wind Velocity 50 m/s with angle of wind 0 degree.

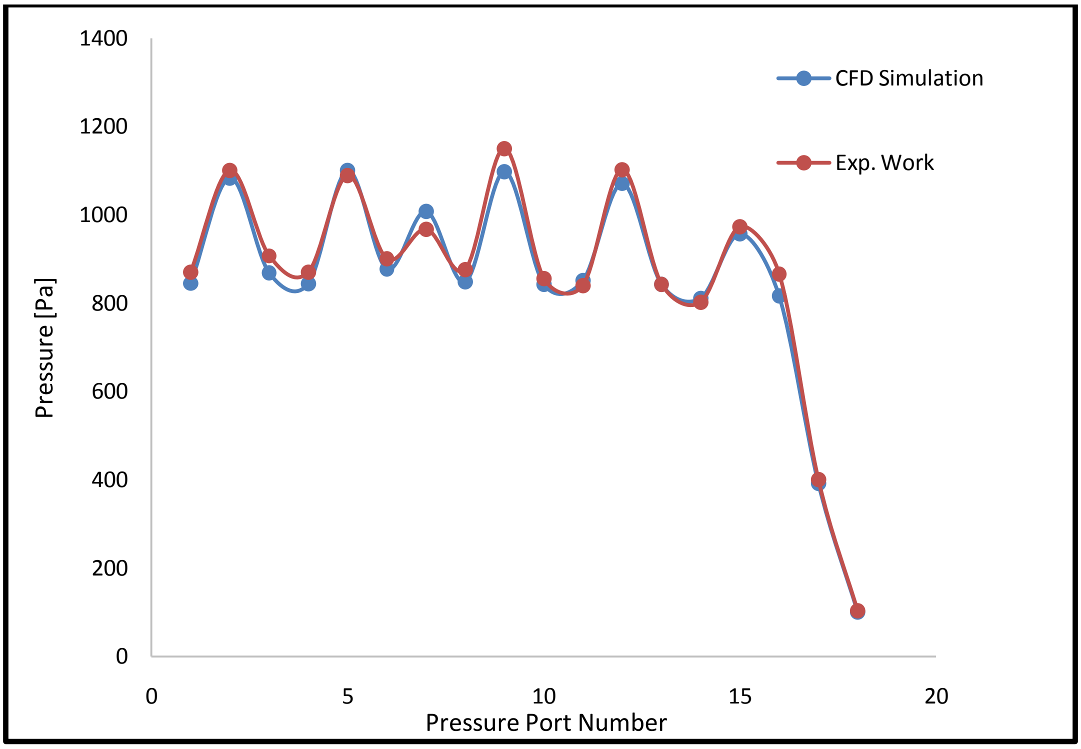

Figure (12) Comparison between Pressures Obtained by Experimental and Numerical Models for Windward2 Model for Wind Velocity 30 m/s with angle of wind 90 degree.

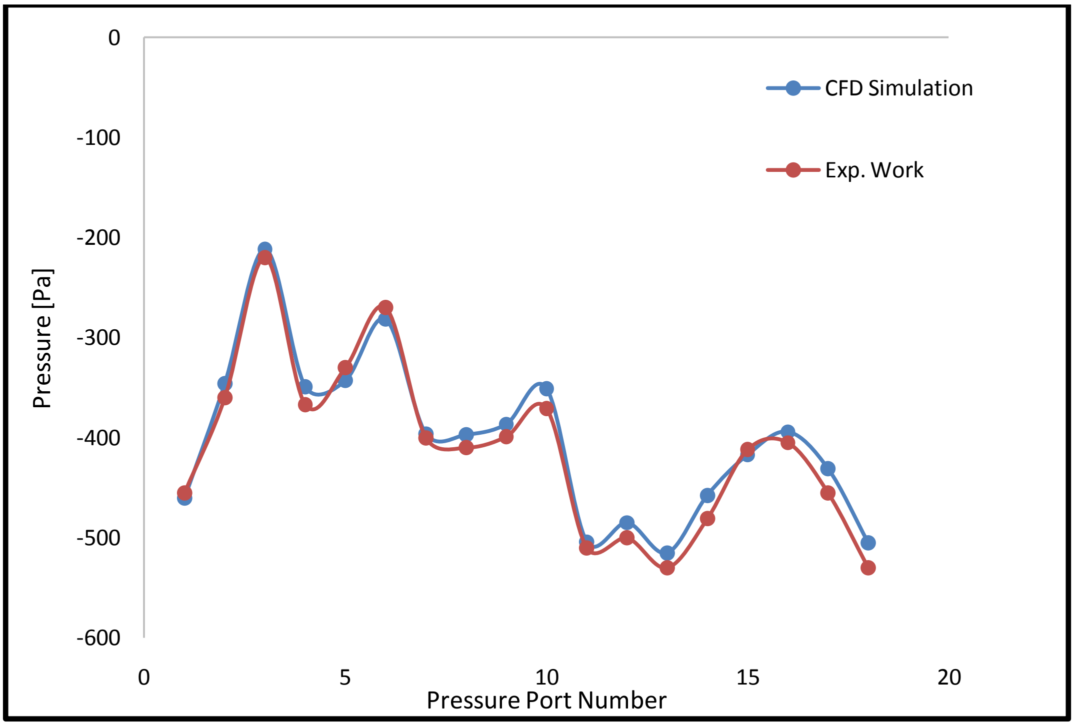

Figure (13) Comparison between Pressures Obtained by Experimental and Numerical Models for Leeward2 Model for Wind Velocity 30 m/s with angle of wind 90 degree.

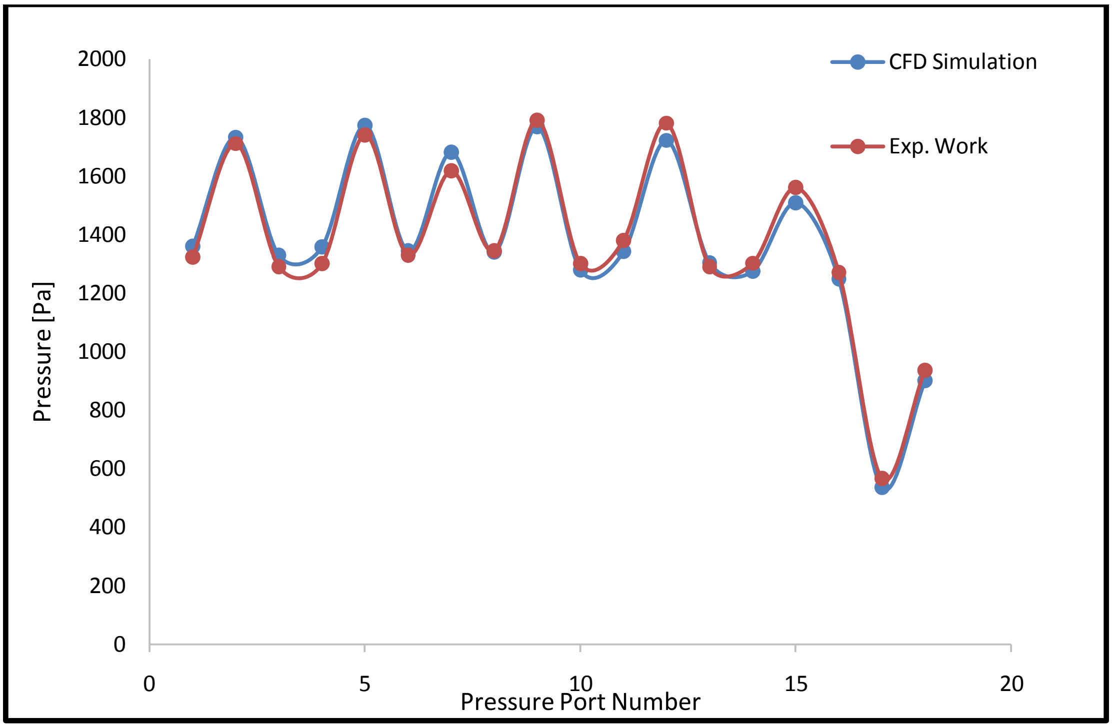

Figure (14) Comparison between Pressures Obtained by Experimental and Numerical Models for Windward2 Model for Wind Velocity 40 m/s with angle of wind 90 degree.

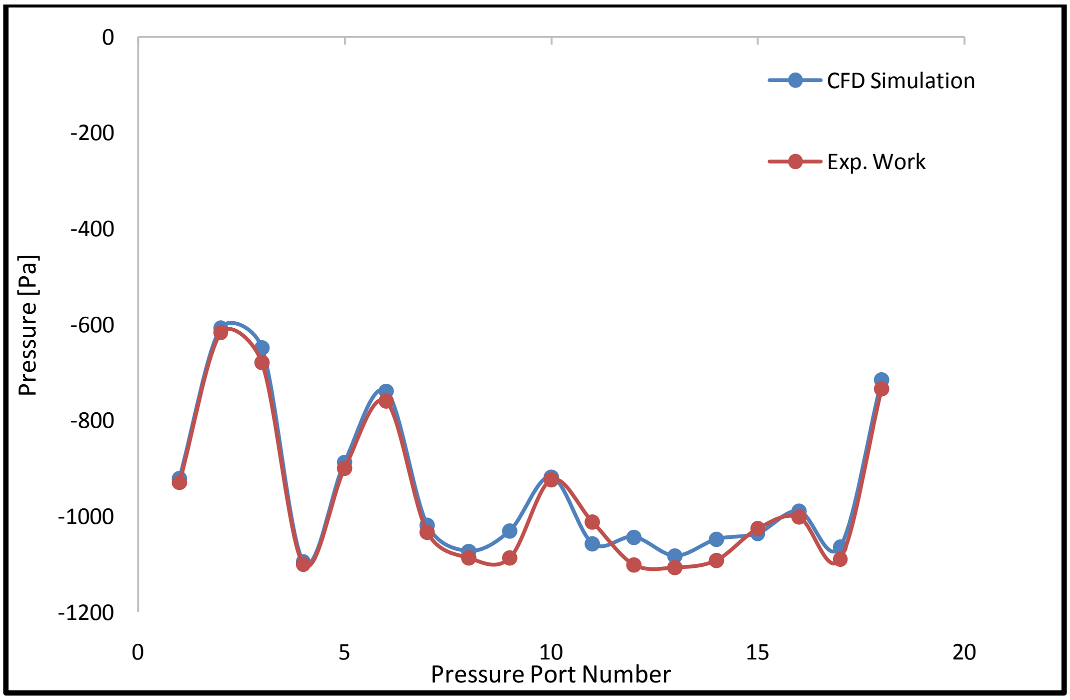

Figure (15) Comparison between Pressures Obtained by Experimental and Numerical Models for Leeward2 Model for Wind Velocity 40 m/s with angle of wind 90 degree.

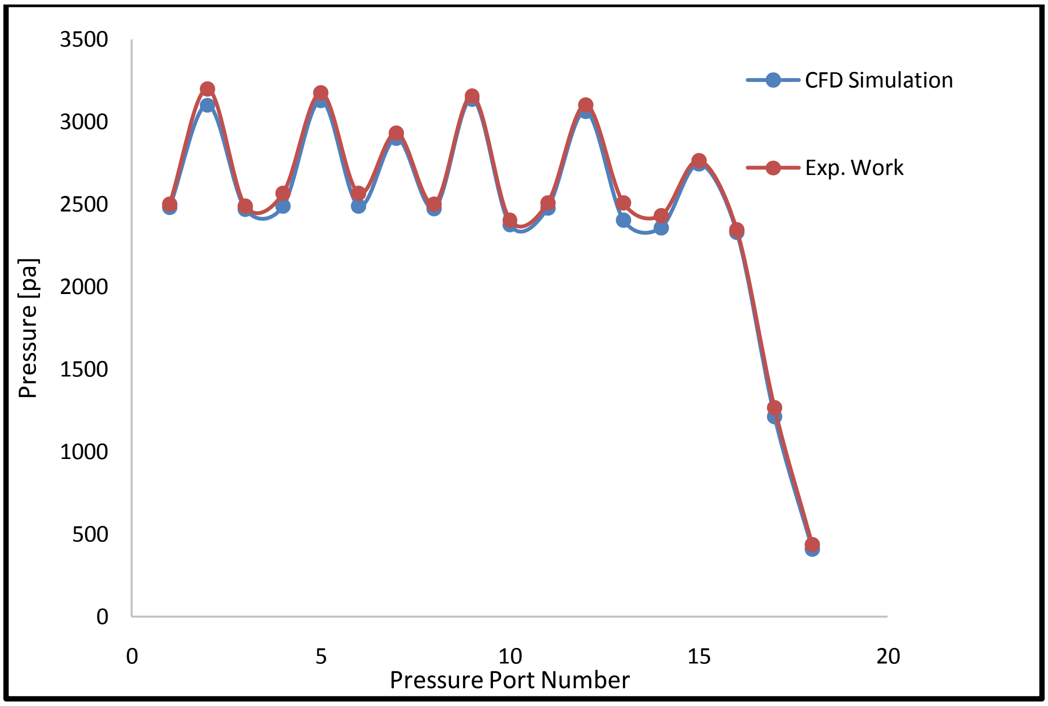

Figure (16) Comparison between Pressures Obtained by Experimental and Numerical Models for Windward2 Model for Wind Velocity 50 m/s with angle of wind 90 degree.

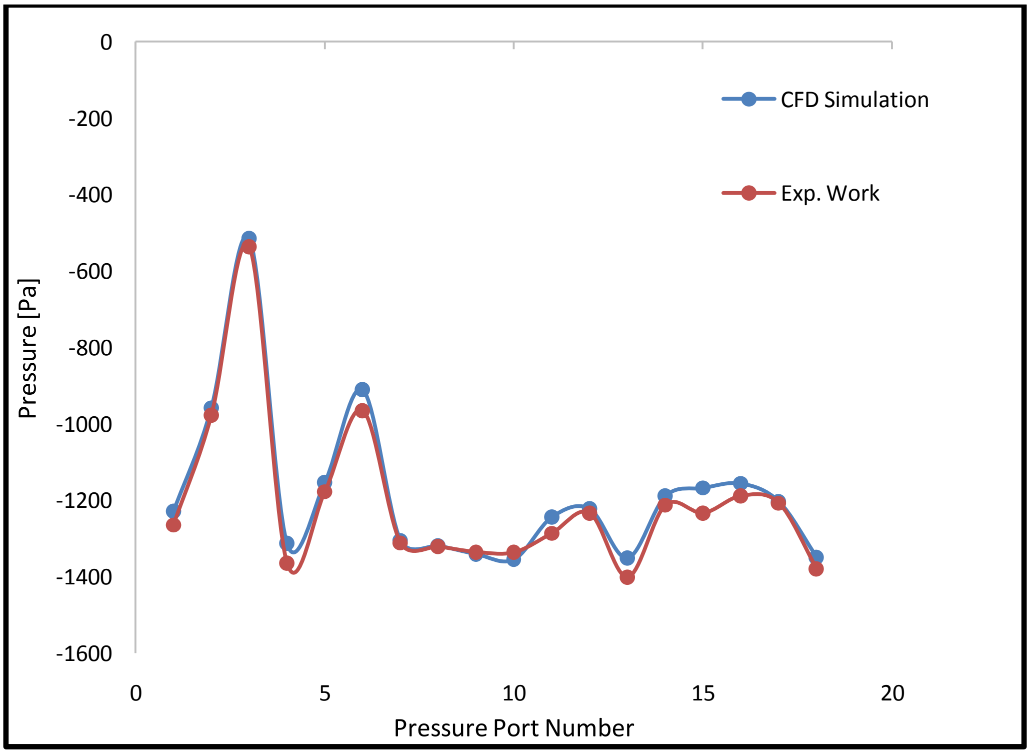

Figure (17) Comparison between Pressures Obtained by Experimental and Numerical Models for Leeward2 Model for Wind Velocity 50 m/s with angle of wind 90 degree.

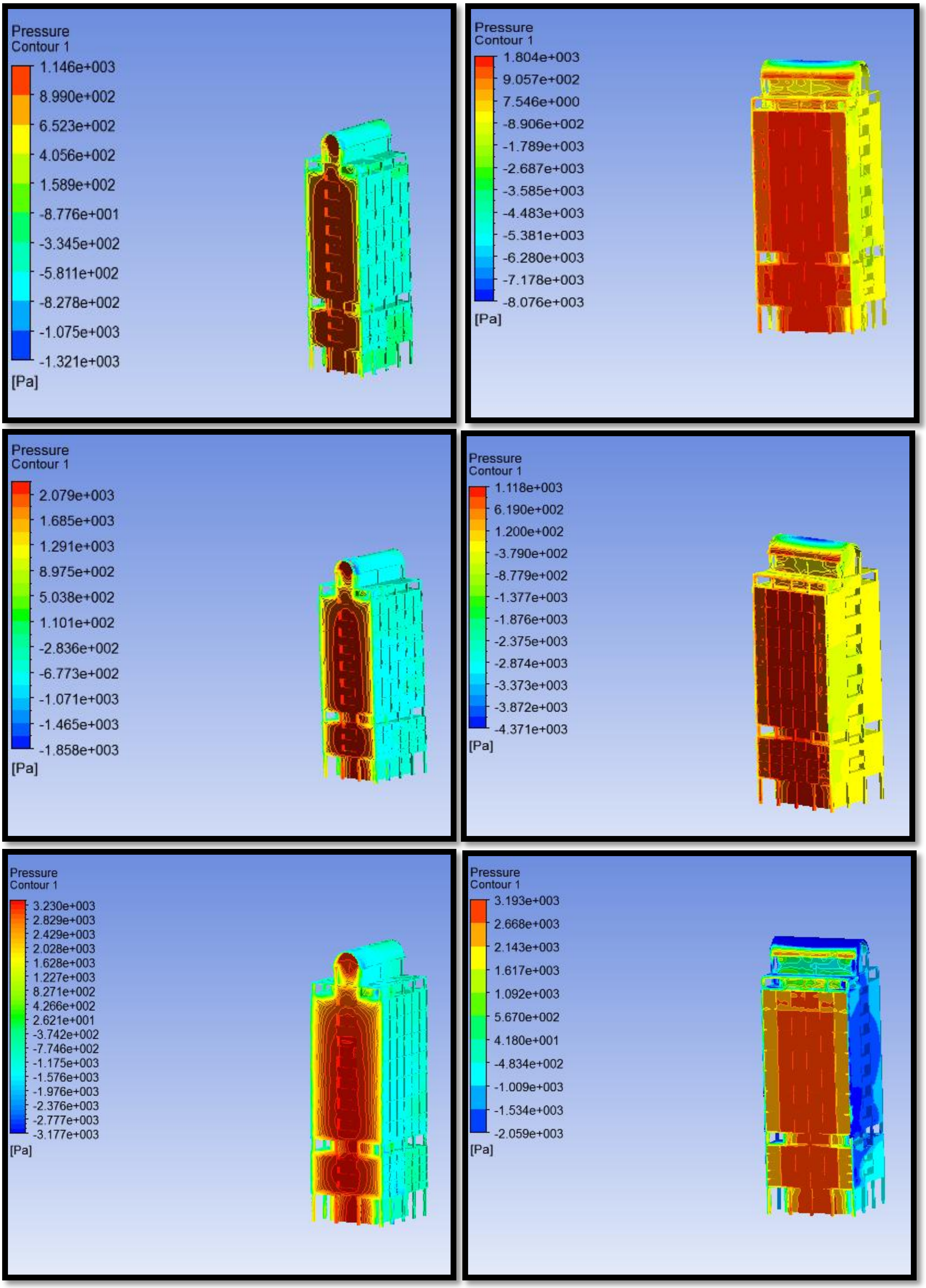

Figure (18) Pressure Contour Results for Model for Deferent Velocity and wind angle.

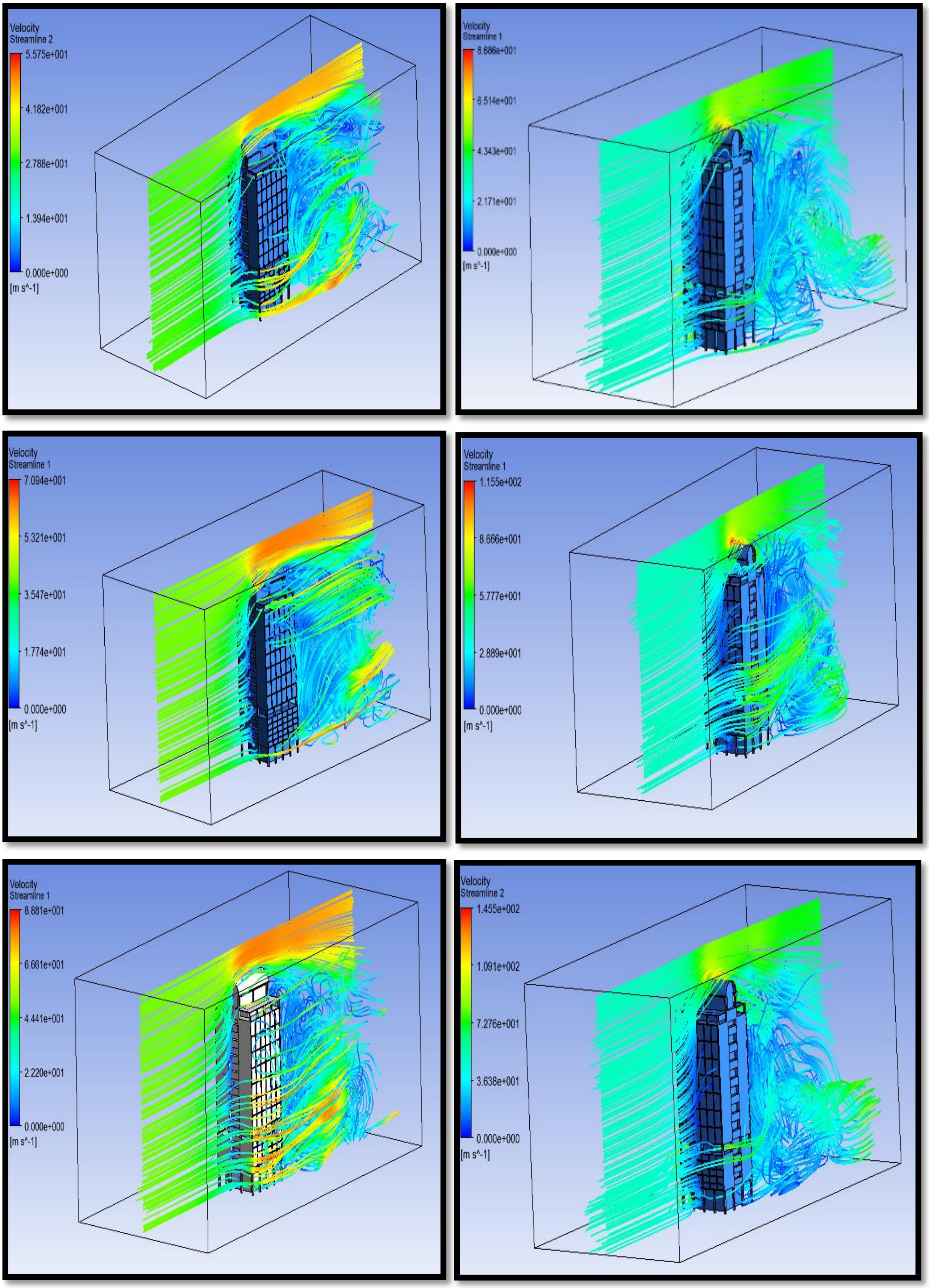

Figure (19) Streamline Velocity Results for Model for Deferent Velocity and wind angle.

Conclusion

In this, paper the pressure results comparison between the CFD simulation and wind tunnel test shows that:

1- The process of comparing the results of pressure showed a very good agreement between the CFD and wind tunnel pressure results.
2- The CFD simulation results can also be used as a substitute for a costly wind tunnel test.
3- TheCFD simulation can show a better picture of the results than the wind tunnel test.
4. The CFD simulation can check any model, no matter how complicated, compared to the wind tunnel.
5. It is also possible to apply any wind speed in the simulation, no matter big or small compared to the wind tunnel.

References

[1.] Inc. ANSYS. (2013). ANSYS FLUENT Theory Guide. Release 18.2, 15317(November), 373–464.

[2.] Jeong, J., & Choi, C.-K. (2008). Comparison of Wind Loads on Buildings using Computational Fluid Dynamics, Design Codes,\rand Wind Tunnel Tests. The fourth International Conference on Advances in Wind and Structures (AWAS'08), (May 2008).

[3.] Paterson and Colin Apelt. (1986). "Computation of wind flows over three-dimensional buildings." Journal of Wind Engineering and Industrial Aerodynamics 24(3), 193–213.

[4.] Rajkamal. D.V.V. & Raviteja. Ch. (2016). Analysis of Wind Forces on a High-Rise Building by RANS-Based Turbulence Models using Computational Fluid Dynamics. (09), 28–34.

[5.] Smith Brayan Stafford and Coull Alex. (1991). Tall Building structures: Analysis and Design.

[6.] Simiu, E., Scanlan, R. H. (1978). Wind Effects on Structures, John Wiley & Sons, New York, N.Y.

[7.] Stathopoulos and Zhou. (1995). "Numerical evaluation of wind pressures on flat roofs with the k-ε model." Building and Environment, Volume 30(Issue 2), Pages 267-276.

[8.] Ton Thi Tu Anh. Modeling of Wind Load on Tall Buildings Using CFD, National University of Singapore. , (2004).

[9.] Weerasuriya, A. U. (2014). Computational Fluid Dynamic (CFD) simulation of flow around tall buildings. Engineer: Journal of the Institution of Engineers, Sri Lanka, 46(3), 43.

[10.] Wijesooriya, K. and Mohotii, D. (2017). A validated Numerical Approach in Wind Design of Supper Tall Buildings.

[11.] Yakhot, V., Orszag, S. A., Thangam, S., Gatski, T. B., & Speziale, C. G. (1992). Development of turbulence models for shear flows by a double expansion technique. Physics of Fluids A, 4(7), 1510–1520.